Molecular Catalysis 502 (2021) 111404

Contents lists available at ScienceDirect

Molecular Catalysis

journal homepage: www.journals.elsevier.com/molecular-catalysis

A robust and stereocomplementary panel of ene-reductase variants for gram-scale asymmetric hydrogenation

Nathalie Nett [a,*], Sabine Duewel [a], Luca Schmermund [a], Gerrit E. Benary [a], Kara Ranaghan [b], Adrian Mulholland [b], Diederik J. Opperman [c], Sabrina Hoebenreich [a]

[a] Fachbereich Chemie, Philipps-Universität Marburg, 35032 Marburg, Germany
[b] Center for Computational Chemistry, School of Chemistry, University of Bristol, Bristol BS8 1TS, UK
[c] Department of Biotechnology, University of the Free State, Bloemfontein 9300, South Africa

ARTICLE INFO

Keywords:
Biocatalysis
Biphasic
Stereoselective
Old yellow enzyme
Protein-ligand docking

ABSTRACT

We report an engineered panel of ene-reductases (ERs) from *Thermus scotoductus* SA-01 (*Ts*ER) that combines control over facial selectivity in the reduction of electron deficient C=C double bonds with thermostability (up to 70 °C), organic solvent tolerance (up to 40 % v/v) and a broad substrate scope (23 compounds, three new to literature). Substrate acceptance and facial selectivity of 3-methylcyclohexenone was rationalized by crystallisation of *Ts*ER C25D/I67T and *in silico* docking. The *Ts*ER variant panel shows excellent enantiomeric excess (*ee*) and yields during bi-phasic preparative scale synthesis, with isolated yield of up to 93 % for 2*R*,5*S*-dihydrocarvone (3.6 g). Turnover frequencies (TOF) of approximately 40 000 h^{-1} were achieved, which are comparable to rates in hetero- and homogeneous metal catalysed hydrogenations. Preliminary batch reactions also demonstrated the reusability of the reaction system by consecutively removing the organic phase (*n*-pentane) for product removal and replacing with fresh substrate. Four consecutive batches yielded ca. 27 g L^{-1} *R*-levodione from a 45 mL aqueous reaction, containing less than 17 mg (10 μM) enzyme and the reaction only stopping because of acidification. The *Ts*ER variant panel provides a robust, highly active and stereocomplementary base for further exploitation as a tool in preparative organic synthesis.

1. Introduction

Significant progress has been made over the past decade in biocatalytic reduction reactions [1,2]. One of these important reactions is the asymmetric transfer hydrogenation of activated C=C bonds, which is catalysed by ene-reductases (ERs) from the Old Yellow Enzyme family (OYE, EC 1.6.99.1). ERs are highly chemo-, regio- and stereoselective due to precise positioning of the substrate via hydrogen bonds and van-der-Waals interactions, allowing an overall trans addition of a hydride and a proton, employing NAD(P)H as hydride source via a flavin cofactor [3–6].

Asymmetric alkene hydrogenation is one of the most widely used industrial reactions, which is still dominated by transition metal catalysis [7]. Access to both stereoisomers with chemical catalysis is achieved using the mirror image of the ligand. This is in stark contrast to enzyme catalysis, where access to both stereoisomers is a major challenge in catalyst development. Although wild types (wt) of recombinant ERs have been intensively studied and include some impressive examples of large-scale syntheses [8–13], the core problem of controlling the facial selectivity of the reduction remains. Excellent stereoselectivities for both isomers are only accessible for a handful of substrates [8,14,15], as almost all wild-type ERs show the same stereopreference [16]. Alternatively, substrate-based stereocontrol, starting from either the *E*- or *Z*-alkene, may give access to both stereoisomers [17]. While protein engineering of ERs has created pairs of stereocomplementary variants for specific compounds [18–23], little is known about their synthetic usefulness, i.e. if they are generally stereocomplementary, about their substrate scope, solvent and thermal stability, or productivity in large scale reactions.

We have previously described stereocomplementary pairs of engineered variants for three compounds from the thermostable ER of *Thermus scotoductus* SA-01 (*Ts*ER/*Ts*OYE). Opposite stereoselectivity, or facial selection, was achieved during the reduction of 3-methylcyclohexenone and methyl-2-(hydroxymethyl)-acrylate with *Ts*ER variant C25D/I67T and (*S*)-carvone with *Ts*ER variant C25G/I67T [24]. Here we expand on these variants and present a small panel of engineered *Ts*ERs,

* Corresponding author.
E-mail address: nathalie.nett@gmail.com (N. Nett).

https://doi.org/10.1016/j.mcat.2021.111404
Received 13 December 2020; Received in revised form 1 January 2021; Accepted 4 January 2021
Available online 21 January 2021

with convenient catalytic characteristics for organic synthesis. This not only includes high activity and stereoselectivity, but also easy production, handling and storage of the catalyst as well as a simple but flexible reaction procedure. Benchmarking tests reveal that this panel combines a broad substrate scope, tolerance to organic solvents and high temperature with convenient catalyst handling. We demonstrate that this combination of properties enables convenient gram-scale synthesis with excellent yields for poorly water-soluble compounds. Importantly, exceptional control over facial selectivity was achieved for half of the substrates.

2. Experimental

Compounds **1a, 2a, 4a-10a**, **12a-14a**,**16a**, **19a, 20a, 24-26, 30-32, 34-36** were obtained from Sigma Aldrich, Alfa Aesar, TCI or Acros. Compounds **3a**, **15a**, **29** and **33** were received as gifts and synthesis is described by the original authors. Compounds **11a**, **17a**, **18a**, **21a - 23a**, **27** and **28** have been synthesized according to the literature, with details given in SI.

2.1. TsER variant creation and biocatalysts production

*Ts*ER variants were created using the megaprimer PCR method as reported before [24] using either *Ts*ER_C25D (5′-GTCCCCCA TGGACCAGTACTCC-3′) or *Ts*ER_C25G (5′-GTCCCCCATGGGTCAGTA CTCC-3′) as forward primers and *Ts*ER_I67T (5′- CATA-AGGGCTGGTACGACCCAAAG-3′) *Ts*ER_I67V (5′-CATAAGGGCTCAC ACGACCCAAAG-3′) *Ts*ER_I67C (5′-CATAAGGGCTGCAACGACCCA AAG-3′) as reverse primers. Heterologous expression and purification by heat treatment was performed as previously reported [24]. Briefly *Ts*ER variants were heterologous expressed in *E. coli* BL21(DE3)ΔnemA [25] using pET22b(+) based gene constructs. After heat purification, *Ts*ER variants were incubated with an excess of FMN for 90 min in the dark at 22 °C, prior to dialysis against 100 mM potassium phosphate buffer (pH 7.4) at 4 °C. Purity of proteins was confirmed by SDS-PAGE (Fig. S1) and enzymes were lyophilized and stored at −20 °C until further use. The amount of ER were determined after dissolving the lyophilized powder before a reaction absorption at 455 nm using the reported extinction coefficient of YqjM ($\varepsilon = 11\ 600\ M^{-1}\ cm^{-1}$) [26].

For *Bs*GDH, the gene construct pACYC-gdh (*Bacillus subtilis* 168 glucose dehydrogenase variant E170K/Q252L) [27] was transformed into *E. coli* BL21-Gold DE3. Expression was performed using TB medium containing 35 mg L^{-1} chloramphenicol in baffled flasks at 37 °C (200 rpm) until the OD_{600} reached 0.4−0.6 IPTG was added to a final concentration of 1 mM and the temperature was reduced to 30 °C. The cultures were incubated overnight, harvested (4480 *xg*, 4 °C, 15 min) and resuspended in KPi buffer (100 mM, pH 7.4). Cells were lysed by sonication on ice (5 × 30 s, 30 s intervals, 5 × 10 cycles, 40 % power, Bandelin Sonoplus HD 2070 with a SGH 213G booster horn and a titanium flat tip (TT13)) and the supernatant was recovered by centrifugation (29 819 *xg*, 4 °C, 45 min). The cleared lysate was purified by incubation at 60 °C for 1 h. After centrifugation (29 819 *xg*, 4 °C, 45 min) the supernatant was lyophilised and stored at −20 °C. Glucose dehydrogenase (GDH-60) was obtained from Evocatal.

2.2. Protein crystallization, X-ray structure determination and docking analysis

Heat purified *Ts*ER C25D/I67T was concentrated through ultrafiltration (30 kDa NMWL, Amicon) with additional FMN added to ensure full occupancy. The protein was further purified using size exclusion chromatography [Sephacryl S100HR (GE Healthcare)] and eluted in 10 mM MOPS buffer (pH 7.4) containing 20 mM NaCl. Crystals of *Ts*ER C25D/I67T were grown using sitting-drop vapour-diffusion in 1 μL drops consisting of equal volumes of 8 mg mL^{-1} *Ts*ER C25D/I67T and crystallization solution (15 % v/v 2-propanol, 0.1 M sodium citrate tribasic dihydrate pH 5.0, 10 % w/v polyethylene glycol 10,000) at 289 K. Crystals were soaked in reservoir solution containing 30 % glycerol prior to cryocooling. X-ray diffraction data were collected at Diamond (UK) on beamline i03. Data was processed using MOSFLM [28] and POINTLESS, with intensities scaled and merged using SCALA [29]. Molecular replacement was performed using Phaser [30] with *Ts*ER wt (PDB 3HF3) as search model. Refinement was performed through iterative cycles of manual model building in COOT [31] and restrained refinement using Refmac [32]. The structure was validated using programs within the CCP4 suite [33] and coordinates and structure factors have been deposited in the Protein Data Bank (PDB) under accession code 5NUX (Table S1).

The crystal structures of *Ts*ER (wt) in complex with *p*-hydroxybenzaldehyde (PDB: 3HGJ) [34] was used in conjunction with the *Ts*ER C25D/I67T variant for docking analysis. The protein was prepared using the Protein Preparation Wizard from Maestro, version 11.0, Schrödinger LLC. For all calculations the dimer structure was retained. Protonation states for titratable amino acids were assigned based on the most favourable interactions with neighbouring residues and the PROPKA program. The His172 and His175 residues were protonated at both epsilon and delta nitrogen atoms, to enable hydrogen bond formation to the substrate. All water molecules and co-crystallized ligands were removed, with the exception of the oxidized FMN cofactors. The oxidized FMN cofactor was converted to the reduced FMNH2 using Antechamber. Substrate **1a** was built in Maestro and prepared for docking using the LigPrep program, version 4.0, Schrödinger LLC and docked into the active site of reduced *Ts*ER wt and C25D/I67T using the Glide docking protocol for Rigid body docking (RGB) with Standard Precision settings or using the Induced fit docking (IFD) protocol within the Schrödinger suite.

2.3. Biotransformations: screening scale

All reactants were mixed in 1.5 mL reaction tubes containing (final concentrations) 100 mM glucose, 10 μM enzyme, 0.1 mM $CoCl_2$, 0.25 mM $NADP^+$, GDH-60 (2.2 U mL^{-1}) and 10 mM substrate (from 1 M stock in EtOH). The reactions were performed at least in triplicates in total reaction volume of 200 μL at 30 °C and 700 rpm in a Thermomixer (Eppendorf). To stop the reaction, the aqueous solution was extracted with 200 μL ethyl acetate. Conversion and enantiomeric excess was determined by GC or HPLC. Peaks were assigned based on available authentic standards, by mass analysis or full characterisation. Precise *ee* determination for low conversion levels was performed as previously described [24]. The optical rotation of 2-methylcyclopentan-1-one (**13b**) was determined to assign chirality. All reactants were mixed in a 50 mL reaction containing 45 mL KPi buffer (100 mM, pH 7.4), glucose (87.5 mM), $NADP^+$ (0.25 mM), *Bs*GDH (2.2 U mL^{-1}) and *Ts*ER C25G/I69T (20 μM). Reaction started upon addition of 50 mM 2-methylcyclopenten-1-one (**13a**) with 5 mL *n*-pentane and was performed at 30 °C and 200 rpm. After completion the whole reaction mixture was extracted with *n*-pentane and the solvent was carefully evaporated under vacuum. The optical rotation was measured with a 20 mg mL^{-1} solution in chloroform in a 50 mm cuvette with a polarimeter P800-T, KRÜSS with λ =589 nm at 25 °C and result in $[\propto]_D^{25}$ -81° indicating that 2*R*-methylcyclopentanone is formed according to Shimoda et al. [35].

2.4. Biotransformations: 20–500 mL scale

3-Methyl-cyclohexanone (**1b**): All reactants were mixed in a 100 mL Schott bottle (50 mL reaction volume) with 45 mL KPi buffer (100 mM, pH 7.4) containing glucose (100 mM), $NADP^+$ (0.25 mM), *Bs*GDH (2.2 U mL^{-1}), 0.1 mM $CoCl_2$, *Ts*ER variant (10 μM), 3-methylcyclohexenone (**1a**, 50 mM) and 10 % (v/v) *n*-pentane. The reaction was performed at 30 °C and shaking (150 rpm). To monitor conversion, 20 μL samples were taken from the *n*-pentane phase and diluted with 200 μL *n*-pentane

for analysing via GC. Upon complete conversion, the whole reaction mixture was extracted three times with 20 mL DEE. The combined organic phases were washed with brine, dried over $MgSO_4$ and the solvent was carefully evaporated under vacuum. Compound *S*-**1b** was further purified using flash column chromatography (*n*-pentane/EtOAc 25:1).

(*R*)-Levodione (**8b**): All reactants were mixed in a 100 mL Erlenmeyer flask (20 mL reaction volume) containing KPi buffer (100 mM, pH 7.4): glucose (500 mM), $NADP^+$ (0.41 mM), *Bs*GDH (2.2 U mL^{-1}), *Ts*ER C25D/I67T (10 μM), ketoisophorone (**8a**, 125 mM) and 10 % (v/v) diisopropylether (DIPE). The reaction was performed at 30 °C and shaking (150 rpm). 100 μL samples were taken and extracted with 100 μL EtOAc for analysing via GC. After completion (91 % conversion) the whole reaction mixture was extracted twice with 20 mL EtOAc. The combined organic phases were washed with brine, dried over $MgSO_4$ and the solvent was evaporated under vacuum.

2-Methyl-5-(prop-1-en-2-yl)cyclohexan-1-one (**9b**): All reactants were mixed in a 300 mL Erlenmeyer flask (100 mL reaction volume) containing KPi buffer (100 mM, pH 7.4), glucose (82.8 mM), $NADP^+$ (2 mM), GDH-60 (2.2 U mL^{-1}), *Ts*ER variant (3.4 μM), carvone (**9a**, 69 mM). The reaction was performed at 30 °C with shaking (110 rpm). 100 μL samples were taken and extracted with 200 μL EtOAc for analysing via GC. After completion the whole reaction mixture was extracted twice with 100 mL EtOAc. The combined organic phases were washed with brine, dried over $MgSO_4$ and the solvent was evaporated under vacuum.

2-Methyl-5-(prop-1-en-2-yl)cyclohexan-1-one (**9b**): All reactants were mixed in a 500 mL Schott bottle (500 mL reaction volume) with 450 mL KPi buffer (100 mM, pH 7.4) containing glucose (100 mM), $NADP^+$ (0.25 mM), *Bs*GDH (2.2 U mL^{-1}), 0.1 mM $CoCl_2$, *Ts*ER variant (5 μM), **9a** (51.2 mM) and 10 % (v/v) *n*-pentane. The reaction was performed at 30 °C with shaking 150 rpm. 20 μL samples were taken from the *n*-pentane phase and diluted with 200 μL *n*-pentane for analysing via GC. After completion the whole reaction mixture was extracted three times with 100 mL DEE. The combined organic phases were washed with brine, dried over $MgSO_4$ and the solvent was evaporated under vacuum.

Ethyl 2-benzyl-3-oxobutanoate (**21b**): All reactants were mixed in a 100 mL Erlenmeyer flask (20 mL reaction volume) in KPi buffer (100 mM, pH 7.4): glucose (500 mM), $NADP^+$ (0.41 mM), GDH-60 (2.2 U mL^{-1}), *Ts*ER C25D/I67T (10 μM), ethyl (*Z*)-2-benzylidene-3-oxobutanoate (**21a**, 50 mM) in 10 % (v/v) diisopropylether (DIPE). The reaction was performed at 30 °C and 100 rpm. 200 μL samples were taken and extracted with 200 μL EtOAc for analysing via GC. After completion (81 % conversion) the whole reaction mixture was extracted twice with 20 mL EtOAc. The combined organic phases were washed with brine, dried over $MgSO_4$ and the solvent was evaporated under vacuum. The product was cleaned via column chromatography (*n*-pentane/EtOAc 10:1).

2.5. Sequential biphasic batch reaction

All reactants were mixed in a 50 mL reaction tube with 45 mL KPi buffer (200 mM, pH 7.4) containing $NADP^+$ (0.27 mM), C25D/I67T (10 μM), glucose (100 mM) and *Bs*GDH (2.2 U mL^{-1}). 5 mL *n*-pentane was added containing 0.5 M **8a**, to yield a final concentration of 50 mM **8a** within the biphasic system (50 mL). The reaction was incubated at 30 °C and 110 rpm. The reaction was monitored by GC. When the reaction completed or stopped, phases were separated by centrifugation (4000 rpm, 15 °C) and a fresh amount of glucose and organic solvent containing **8a** was added.

3. Results and discussion

All enzyme variants reported in this study are easily separated from *E. coli* host proteins by heat treatment for 90 min at 70 °C [24,36]. Enzyme preparations were reconstituted with FMN followed by dialysis, yielding approximately 110−130 mg purified enzyme per litre of *E. coli* culture. We found that shock-frozen catalyst solutions maintained their activity when stored at −20 °C for over a year, with only repetitive thawing and freezing having negative effects. To overcome this limitation, we produced freeze-dried powders, which offer advantages upon storage and handling.

3.1. Substrate scope

To expand on our earlier work uncovering the stereocomplementarity of variants C25D_I67T and C25G of *Ts*ER [24], we decided to further explore the active site architecture by modifying residue I67. A panel of *Ts*ER variants was created by mutating I67 to either a Val, Thr or Cys into variants C25D and C25G. The engineered *Ts*ER variants and the wild-type enzyme (wt) were tested against a total of 38 electron-poor alkenes, which included 3-methylcylcohexenone (**1a**), (*S*)-carvone (**9a**) and methyl-2-(hydroxymethyl)-acrylate (**17a**) previously reported on [24]. This benchmarking set of substrates contained cyclohexenones and cyclopentenones, α,β-unsaturated linear alkenones and alkenals, acrylesters, nitroalkenes, a maleimide, citronellylnitrile, two alkynals and an alkynone (Schemes 1 and S1).

A total number of 23 compounds were reduced at the C═C bond (Scheme 1), introducing new stereocenters with high stereoselectivity (Table 1). Access to both stereoisomers was observed for 11 substrates (**1a**-**4a**, **6**-**7a**, **9a**, **14**-**15a**, **17a**, **22a**) with stereoselectivities ranging from 17 to >99 % *ee*. This represents a broad control over the facial selectivity for a single set of ER variants. In eight additional cases (**8a**, **10**-**13a**, **18**-**19a**, **21a**) high chiral purity (88 to >99 % *ee*) for one stereoisomer was obtained. Comparable conversions were observed with the wt as previously reported [2], but the differences in reaction conditions lead to a 40 % increase in citral reduction. Also, the use of 10 % v/v organic solvents suppressed background racemisation of stereocenters, especially for **13b**. The stereochemical outcome of **13a** reduction using *Ts*ER, previously reported to be *S* [15,36,37], was unambiguously corrected to be *R* by optical rotation.

In addition, excellent conversions up to >99 % were achieved under screening conditions (Table 1). Originally, these mutations were evolved for cyclohexanone derivatives [24,38], therefore it is particularly interesting that structures such as **17**-**19a** as well as derivatives of cinnamic acid (**20**-**23a**) are accepted with excellent conversions. These compounds are valuable building blocks of industrial synthons, fragrance and flavour substances. Besides typical ER substrates, several new compounds for ERs were tested of which three were transformed (**4b**, **16b**, **21b**). We noted that kinetic resolution of **4a** occurred and produced a compound with >99:1 *dr*. C25D based variants consume the opposite enantiomer of **4a** than C25G based variants. Nevertheless, due to the C2-symmetry of **4b**, the same meso isomer is formed (Scheme S2). Reduction of compound **16a** creates two new stereocenters with >99:1 *dr*.

3.2. Structural characterization

One of the most promising stereocomplementary variants (C25D/I67T) was selected for structural investigation. No significant differences could be observed in the main chain conformation in the active site as compared with the wt structure (Fig. S2). The side chain of D25 adopts a conformation that is rotated away from the oxidized FMN and increases marginally the active site volume together with the I67T replacement. Numerous attempts however to co-crystallize C25D/I67T with different substrates to evaluate binding orientations were unsuccessful. We therefore turned to *in silico* experiments and analysed the interactions for **1a** with the wt and C25D/I67T variant using both rigid body docking (RBD) and induced-fit docking (IFD). **1a** was selected as it not only showed a reversal of facial selection, but also a dramatic increase in activity [24]. The structures were prepared with a reduced FMN cofactor to mimic the active state and the potential substrate anchors (H172 and H175) were fully protonated, to enable hydrogen bonding. Fig. 1 shows

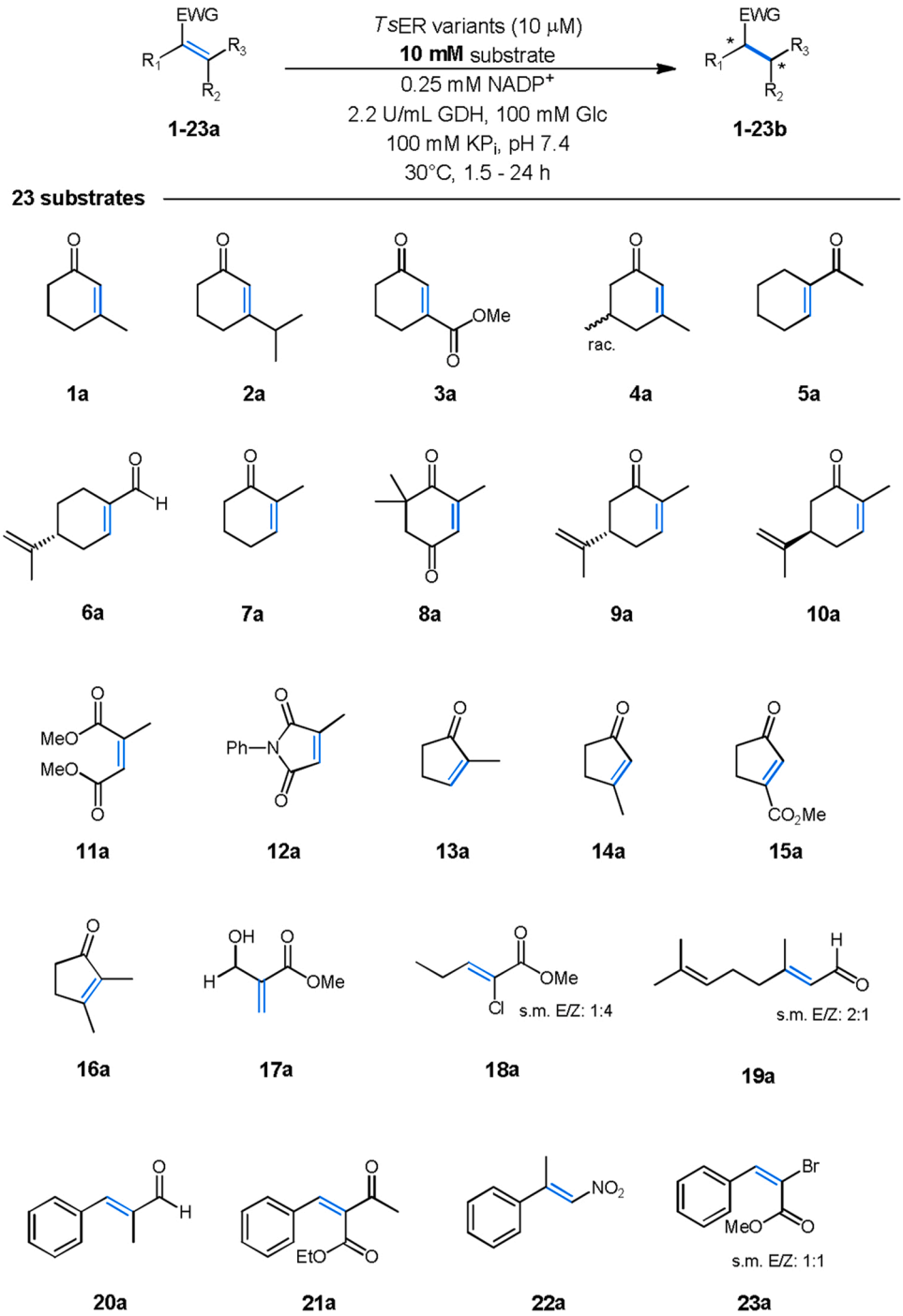

Scheme 1. Substrate scope of the *Ts*ER panel. rac: racemic; s.m.: starting material.

an overlay of the best RBD and IFD pose for the wt (A) and C25D/I67T (B). Binding poses were considered as productive when the hydride transfer angle ranges from 80 to 120° and the distance (H to Cβ) shorter than 4.85 Å [19,39]. The hydride attack angles and distances improve in both cases with IFD. Now, productive poses in the wt unambiguously predict the experimentally observed *S*-selectivity (76 % *ee*) and *R*-selectivity (93 % *ee*) for the C25D/I67T variant, due to a "flipped" binding mode (Tables S2 and S3). The improved predictions from IFD originate from a side chain flip of residue 67 and rearrangements of side chains Y27, H172 and Y177. The imidazole ring of H172 rotates by 90° in the wt, an effect that was also observed *in crystallo* for OYE1-W116I upon substrate binding [40]. Notably, in C25D/I67T, the phenolic proton of Y177 changes position in the IFD structure, adopting the correct orientation for proton transfer, as shown in the work of Lonsdale et al. [41] and the hydride attack angle has improved from 81.4° to 93.8°. We predict that the more hydrophobic pocket created in the C25G based mutants, allows sufficient space and van-der Waals interactions to host smaller substituents on the Cβ, allowing "normal" binding poses to occur, to give the experimentally determined *S*-selectivity.

3.3. Physicochemical characterization

Encouraged by our initial screening, we investigated the physicochemical limits of our reaction system. The reaction system consists of two enzymes, the ER and a NADPH recycling enzyme (glucose dehydrogenase, GDH) supplying the consumed hydride from glucose.

Table 1
Substrate scope and stereoselectivities of the *Ts*ER variant panel.

Product	wt conv/% *ee*/%	C25D/I67C conv/% *ee*/%	C25D/I67T conv/% *ee*/%	C25D/I67V conv/% *ee*/%	C25G conv/% *ee*/%	C25G/I67C conv/% *ee*/%	C25G/I67T conv/% *ee*/%	C25G/I67V conv/% *ee*/%
1b[a]	1 76*S*	63 94*R*	95 93*R*	98 92*R*	6 >99*S*	6 57*S*	49 74*S*	97 62*S*
2b[*]	n.c	22 99*R*	29 99*R*	32 99*R*	1 n.d.	6 99*S*	36 99*S*	34 99*S*
3b[*]	>99 >99*R*	>99 >99*R*	>99 >99*R*	>99 >99*R*	>99 >99*S*	>99 >99*S*	>99 88*S*	>99 >99*S*
4b	1 rac	46 >99	51 >99	33 >99	10 >99	4 n.d.	53 >99	21 >99
5b[*]	99	99	99	99	85	99	99	99
6b[*,b]	88 83(2)	68 49(2)	84 27 (2)	74 64 (2)	38 57(2)	8 24(1)	25 17(1)	6 17(1)
7b[*]	>99 93*R*	>99 13*S*	>99 5*R*	>99 5*R*	>99 72*R*	>99 18*S*	>99 14*S*	>99 24*S*
8b[c]	>99 90*R*	>99 92*R*	>99 92*R*	>99 92*R*	72 86*R*	25 91*R*	88 88*R*	71 86*R*
9b[d]	>99 91 (2*R*,5*S*) *cis*	>99 92 (2*R*,5*S*) *cis*	>99 92 (2*R*,5*S*) *cis*	>99 93 (2*R*,5*S*) *cis*	86 89 (2*R*,5*S*) *cis*	87 91 (2*S*,5*S*) *trans*	87 88 (2*S*,5*S*) *trans*	90 86 (2*S*,5*S*) *trans*
10b[d]	>99 96 (2*R*,5*R*) *trans*	>99 96 (2*R*,5*R*) *trans*	>99 96 (2*R*,5*R*) *trans*	>99 96 (2*R*,5*R*) *trans*	97 98 (2*R*,5*R*) *trans*	86 95 (2*R*,5*R*) *trans*	98 98 (2*R*,5*R*) *trans*	58 99 (2*R*,5*R*) *trans*
11b[*]	>99 >99*R*	>99 >99*R*	>99 >99*R*	>99[d] >99*R*	38 >99*R*	25 >99*R*	97 96*R*	34 54*R*
12b[*]	97 >99*R*	99 >99*R*	>99 >99*R*	99 >99*R*	>99 >99*R*	>99 >99*R*	>99 >99*R*	>99 >99*R*
13b[*]	99 79*R* 96*R*[e]	99 66*R* 71*R*[e]	91 57*R* 88*R*[e]	99 69*R* 88*R*[e]	90 87*R* 88*R*[e]	>99 84*R* 82*R*[e]	99 81*R* 80*R*[e]	96 85*R* 84*R*[e]
14b	14 94*S*	8 47*R*	9 57*R*	10 37*R*	nc	nc	nc	nc
15b[*]	>99 >99*R*	>99 >99*R*	>99 >99*R*	>99 >99*R*	>99 87*S*	>99 96*S*	>99 90*S*	>99 99*S*
16b	2 n.d.	7 n.d.	2 n.d.	17 n.d.	<1 n.d.	<1 n.d.	2 n.d.	1 n.d.
17b[*]	94 76*R*	96 >99*S*	98 97*S*	83 >99*S*	nc	2 nd	11 79*R*	nc
18b	94 46*S*	35 26*R*	51 5*R*	27 47*R*	7 51*R*	12 99*R*	37 92*R*	36 >99*R*
19b	60 99*S*	52 99*S*	70 99*S*	81 99*S*	31 87*S*	5 86*S*	49 94*S*	14 88*S*
20b	92 rac	85 rac	47 rac	57 rac	97 rac	96 rac	94 rac	98 rac
21b[*]	40 91[e] >99	58 88[e] >99	43 88[e] >99	60 96[e] >99	38 39[e] >99	45 42[e] >99	48 90[e] >99	37 37[e] >99
22b	13 >99*S*	27 >99*S*	28 >99*S*	33 >99*S*	62 >99*R*	51 >99*R*	64 >99*R*	63 >99*R*
23b	4 n.d.	1 n.d.	4 n.d.	10 n.d.	1 n.d.	4 n.d.	3 n.d.	7 n.d.

All reactions were done in triplicates; standard deviation for conversion is ± 5 %. The reaction was stopped after 24 h unless otherwise specified. The numbers in parenthesis for **6b** indicate the major diastereomer based on retention times.

[a] 5 h.
[b] 2 h.
[c] 2.5 h.
[d] 90 min.
[e] 10 % (v/v) MTBE.
[*] Confirmed by GC/MS analysis; s.m. = starting material; rac. = racemic; nc = no conversion, nd = not determined. Control reactions without ER showed no background reduction of C=C or C=O bonds.

First, we investigated the effect of pH on our reaction system (Fig. 2). C25D/I67T is less affected by a change in pH and still shows **8b**-production at pH 10. Remarkably, it is still 40 % active at a pH of 5, especially considering that NADPH/$NADP^+$ rapidly degrades below pH 7 [42]. The glucose based NADPH recycling irreversibly produces gluconic acid as side product, leading to acidification of the reaction [43]. Our 100 mM buffer capacity is ten-times higher than the amount of possible acid equivalents under screening conditions, and ensures a constant pH, even when considering uncoupling through side reactions. We found that up to 200 mM potassium phosphate buffer can be used, especially when aiming for higher substrate loadings (>100 mM, *vide infra*). An alternative would be process engineering to compensate for the pH decrease.

Enzymes with high thermal stability are of particular interest to biotechnology as increased stability and life-times enables more flexibility in process design. Before studying the impact of temperature on our reaction system, we assessed both the ERs and GDHs individually. The commercially available recycling system (GDH-60, Evocatal) was

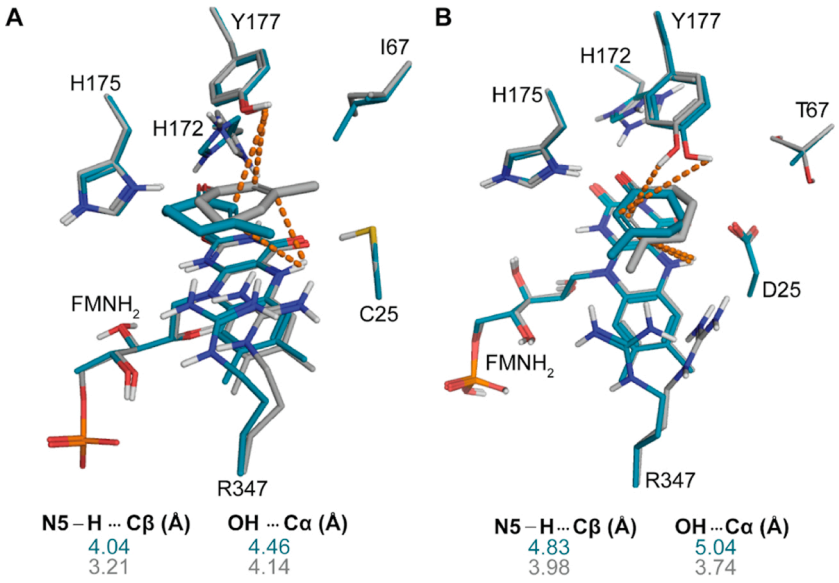

Fig. 1. Comparison of RBD (cyan) and IFD (grey) docking of **1a** in *Ts*ER wt (A) and *Ts*ER C25D/I67T (B).

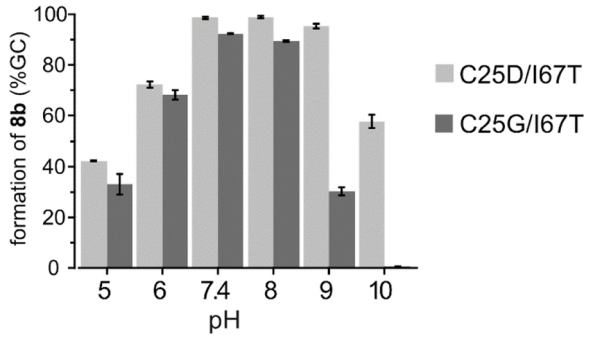

Fig. 2. Effect of pH on productivity. pH profile of **8b**-production with C25D/I67T or C25G/I67T and GDH-60.

found to be active up to 50 °C (Table S6). Thus, we switched to an engineered GDH from *Bacillus subtilis* (*Bs*GDH E170 K/Q252 L) [27,44], which still shows 60 % specific activity at 70 °C under our reaction conditions.

Thermal inactivation of variant C25G/I67T and C25D/I67T was assessed by incubating purified enzymes in buffer at temperatures between 4 and 70 °C for 14.5 h prior to a reaction at 30 °C (Fig. 3A). Both *Ts*ER variants retain full activity up to an incubation temperature of 60 °C. At 70 °C incubation, C25D/I67T lost 3 % and C25G/I67T 14 % of its initial activity. This thermal stability is comparable to that of the wt [45]. Notable is the activity increase of C25G/I67T after pre-incubation at room temperature (22 °C) and above, while the activation effect might be masked for C25D/I67T, since full conversion was reached.

After ensuring thermal stability of both enzymes, the reaction system was tested for levodione (**8b**) production at reaction temperatures between 30 °C and 75 °C. Formation of **8b** completes in 150 min under screening conditions. Increasing the temperature accelerated the reaction, now reaching full conversion in less than 20 min (C25D/I67T) or 40 min (C25G/I67T) at 55 °C (Fig. 3C,D). Productivity was not affected up to 65 °C, while both variants start losing activity above 65 °C. In general, working above 75 °C reduced the lifetime of the reaction system below 20 min. Not only the enzymes, but also the nicotinamide cofactor (NADPH/$NADP^+$) is labile at higher temperatures. The half-life of dissolved NADPH at 70 °C and above is less than 10 min [46]. Therefore, it is impossible to distinguish between cofactor or enzyme degradation as source for lost activity at high temperatures. Consequently, as long as thermolabile cofactors are used, increased reaction temperatures may negatively impact yields for reaction times longer than a few hours, despite the benefits of increased reaction rate and enhanced solubility of organic molecules at higher temperatures.

R-levodione racemizes in buffered aqueous solution approximately 3 % *ee* per hour at ambient temperatures [47,48]. We expected the effect to be more dominant at increased temperature and found that incubation of *R*-**8b** at 65 °C and above for 1 h results in a loss of enantiopurity yielding an *ee* of 8 %. This temperature accelerated racemization is observed when levodione is incubated in buffer, in the presence of the recycling system or in presence of a *Ts*ER variant. When all components of the reaction system are present, *R*-**8b** is produced at 70 °C with an *ee* of 37 % (Fig. 3B). Thus, an increased reaction temperature seems only beneficial for non-racemizable or achiral compounds, but the panel is robust enough to tolerate exposure to elevated temperatures.

3.4. Organic solvent tolerance

We also investigated the effect of organic solvents as a process parameter on the bioreduction. Low water-solubility of most ER substrates represent a considerable challenge, often resulting in low substrate loadings and significant amounts of waste water [1]. Addition of organic co-solvents and use of biphasic reaction systems therefore offer significant advantages, often increasing the biocatalyst performance in synthetic chemistry. We found that water-miscible solvents are tolerated up to 10 % (v/v) without loss of productivity (Fig. 4A,B). Polar solvents like C1 to C3 alcohols, DMSO or acetonitrile, common co-solvents in biotransformation, reduce productivity at 20 % v/v and above. Other ERs have likewise shown a similar intolerance against such co-solvents [11,49,50], but no clear trend is apparent. In contrast, water-immiscible solvents are tolerated without loss of productivity up to a phase ratio of 1:4 (20 % v/v of total reaction volume). In general, a small volumetric amount of organic solvents (5–10 % v/v) already increased **21b** productivity up to 2-fold, enabling full conversion of this poorly water-soluble substrate.

Addition of *n*-pentane, MTBE, diisopropylether (DIPE) or toluene proved to be particularly effective. Due to the low water miscibility of *n*-pentane (39 mg L^{-1}), the enzymes stayed active in all tested phase ratios (max. 2:3 *n*-pentane: buffer) and recovery of a clean product by simple phase separation was possible. Our findings that immiscible solvents are more compatible and enhance conversion are in-line with observations made for other wild-type ERs [49–51].

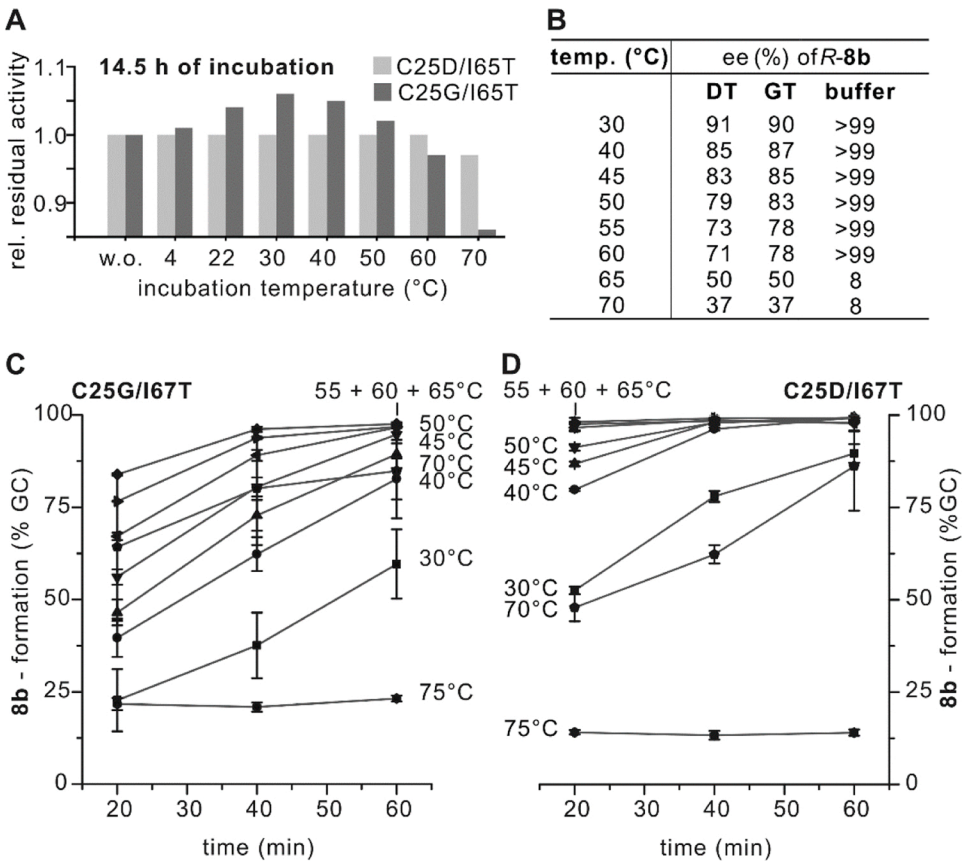

temp. (°C)	ee (%) of *R*-**8b**		
	DT	**GT**	**buffer**
30	91	90	>99
40	85	87	>99
45	83	85	>99
50	79	83	>99
55	73	78	>99
60	71	78	>99
65	50	50	8
70	37	37	8

Fig. 3. Thermostability assessment of the reaction system. A) Residual activity at 30 °C of *Ts*ER C25G/I67T and C25D/I67T after 14.5 h incubation at different temperatures. B) Effect of temperature on the final enantiopurity of **8b**. Values are obtained with three different enzyme batches, ±0.8 % s.d. of *ee*. C and D) Temperature-time dependent formation of **8b** using the engineered *Bs*GDH and C25G/I67T (C) and C25D/I67T (D) at reaction temperatures between 30 and 75 °C.

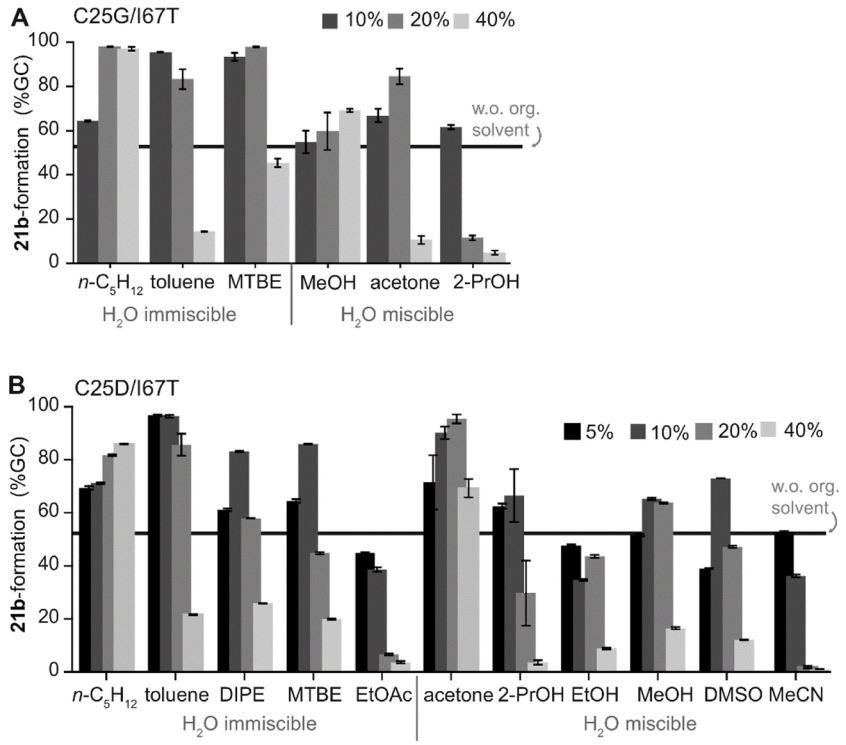

Fig. 4. Effect of organic solvents on *Ts*ER variants C25G/I67T (A) and C25D/I67T (B). The total reaction volume was kept constant; percentages correspond to phase ratios of 1:19, 1:9, 1:4 and 2:3 in biphasic systems.

Table 2
Preparative scale bioreduction using *Ts*ER variants and engineered *Bs*GDH.

Product	*Ts*ER	$V^{a)}$ (mL)	*C* (mM)	Cat. Loading (mol%)	$T^{b)}$ (h)	Conv.(%GC)	*er/dr*	Isolated Yield (%)	TON[c)]	TOF[d)] (h^{-1})
1b[e)]	C25G/I67T	50	50	10 μM (0.02)	8.0	78	76:24 *S*	72[h)] (0.2 g)	3,900	1,986
1b[e)]	C25D/I67T	50	50	10 μM (0.02)	9.0	99	>99:1 *R*	91[h)] (0.26 g)	4,970	3,911
8b[f)]	C25D/I67T	20	125	10 μM (0.008)	1.5	91	99:1 *R*	65 (0.25 g)	11,375	7,583
9b[i)]	C25G/I67T	100	69	3.4 μM (0.005)	4.5	>99	94:6[g)] *trans*	90 (0.94 g)	20,294	5,958
9b[i)]	C25D/I67T	100	69	3.4 μM (0.005)	6.8	>99	98:2[g)] *cis*	78 (0.83 g)	20,294	4,928
9b[e)]	C25D/I67T	500	51	5 μM (0.01)	7.0	>99	98:2[g)] *cis*	93[h)] (3.6 g)	10,189	40,634
21b[f,i)]	C25D/I67T	20	50	10 μM (0.02)	2.0	81	>99:1	76 (0.17 g)	4,050	2,025

a) Volume: Total reaction including both phases.
b) Time until completion of reaction.
c) Turnover numbers (TONs) are defined as mol product (as per GC conversion) formed per mol enzyme upon completion of the reaction.
d) Turnover frequency (TOF) is defined as the mol product (as per GC conversion) formed per mol enzyme per hour. TOFs were determined after 30 min, with the exception of **8b** and **21b**, calculated after 1.5 and 2 h, respectively (time of completion of reaction).
e) 9:1 buffer: *n*-pentane.
f) 9:1 buffer: DIPE.
g) Starting material contains 2 % enantiomer.
h) Extraction with diethyl ether increased yield.
i) Performed with GDH-60 (Evocatal) without second phase.

3.5. Preparative scale reactions

To ultimately prove the high potential of the panel, we performed bioreductions at a preparative scale of between 20–500 mL with selected variants for compounds **1a**, **8a**, **9a** and **21a** at 30 °C (Table 1). Scale-up successfully reproduced conversion and selectivity values observed during screening experiments. We were also able to reduce the amount of glucose from a 10-fold excess to 1.75 molar equivalents. To minimize side reactions, we also limited the available O_2 by reactor design (closed bottles with varying head space). The use of a bi-phasic reaction system increased the enantiopurity of **8b**. The beneficial effect of a biphasic system on enantiopurity has been previously described for compounds prone to racemization, such as **13b** and **8b** [47,52].

Excellent yields of up to 93 % were achieved, demonstrating that our reaction system is easily scaled to gram quantities. Substrate loadings up to 125 mM (19 g L^{-1}) are demonstrated. Catalyst loadings were 100-fold reduced from 0.1 mol%, used during screening and our previous reports on *Ts*ER [24], to 0.02−0.008 mol% resulting in excellent TONs (3,900 to 20,294) with turnover frequencies (TOF) between 1,986 and 40,634 h^{-1}. All reactions were complete in less than 9 h, whereas other preparative scale bioreductions with ERs are reported to run between 20−96 h [9–11] or at 10–40 times higher catalyst loadings [53]. A 500 mL scale bioreduction of **9a** resulted in an isolated yield of 93 % of 2*R*, 5*S*-**9b** (3.63 g). Overall, these examples demonstrate the efficiency of our *Ts*ER variant panel for organic synthesis with space time yields (STYs) ranging between 0.5–8.3 g L^{-1} h^{-1} (Table 2).

3.6. Sequential biphasic batch reaction

As biphasic systems enables enzyme reusability, we performed consecutive batch experiments in which the organic phase containing the substrate (0.5 M **8b** in 5 mL *n*-pentane) was repeatedly replaced after each transformation. This allowed consecutive substrate loadings of 50 mM **8b** to the biphasic system (50 mL) while leaving the enzyme and recycling system in the aqueous phase (45 mL). We achieved four cycles (Fig. 5), with the first two cycles at 90 min each, cycle 3 at 180 min and the final cycle at 205 min. Relative to the aqueous phase, ca. 27 g L^{-1} **8b** were produced before the reactions stopped, with a TTN of more than 17 500. We identified the build-up of stoichiometric amounts of gluconate and a pH drop to 5.2 as cause, also for the reduced productivity over the later batch cycles.

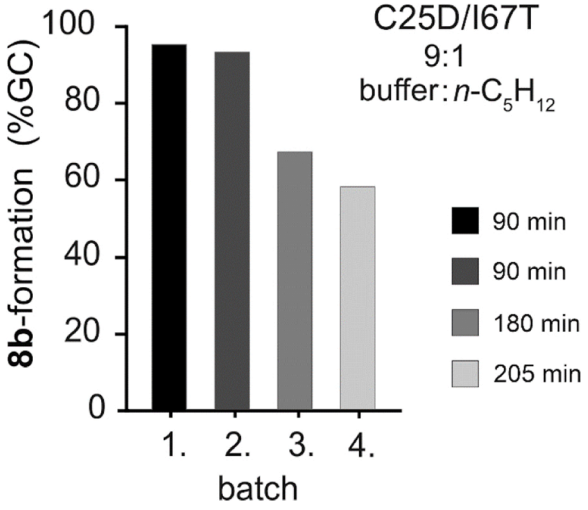

Fig. 5. Consecutive biphasic batch reactions to evaluate reusability of *Ts*ER C25D/I67T for conversion of **8a**. Four consecutive batches in 50 mL volume (1:9, *n*-pentane:buffer) were performed.

4. Conclusions

We present here a robust panel of *Ts*ER variants for asymmetric transfer hydrogenation of a wide range of substrates. The increased substrate scope, broad stereocomplementarity and high enantioselectivities of the panel complements the already established reactions with wild type *Ts*ER [24,36,45].

Our reaction system, consisting of two engineered enzymes, is convenient to prepare and handle and also allows for long term storage as freeze-dried powders. TOF of up to 40,000 h^{-1}, which are comparable to hydrogenation rates by heterogeneous and homogeneous transition metal catalysts were demonstrated at preparative scale. The observed tolerance to organic solvents not only allows working at high substrate loadings, particularly for poorly water-soluble substrates, but also simplifies product recovery and decreases racemization. Non-miscible solvents also allows for sequential batch reactions, whereby product can be removed and the reaction repeated using the same enzymes.

The high activity, robustness and stereocomplementarity demonstrated by the *Ts*ER variant collection, provides a base to further exploit these enzymes as a tool in preparative organic synthesis, especially for cascade and chemo-enzymatic one-pot reactions [54,55]. Moreover, the use of variants of the same ER would reduce efforts during reaction optimization.

Credit author statement

S.H. conceptualized the study. Supervision by S.H., D.J.O. (X-ray structure determination) and A.M. (docking analysis). Investigation, methodology and formal analysis by N.N., S.D., L.S., G.E.B. and K.R. All authors contributed to the writing and editing of the manuscript.

Funding

This work was supported by the LOEWE Research Cluster SynChemBio (Hesse, Germany) and the Philipps-Universität Marburg. The DAAD is acknowledged for the exchange scholarship to N. Nett.

Declaration of Competing Interest

The authors declare that they have no known competing financial interests or personal relationships that could have appeared to influence the work reported in this paper.

Acknowledgements

We thank Manfred T. Reetz for access to instruments, Valérie Alezra and Timo Völker for providing compounds 29 and 33, Monika Ballmann, Alexandra Richter, Saskia Döhring and the mass department for excellent technical assistance as well as the beamline scientists of Diamond Light Source beamline i03 for assisting with data collection under proposal mx12633.

Appendix A. Supplementary data

Supplementary material related to this article can be found, in the online version, at doi:https://doi.org/10.1016/j.mcat.2021.111404.

References

[1] F. Hollmann, D.J. Opperman, C.E. Paul, Biocatalytic reduction reactions from a chemist's perspective, Angew. Chemie Int. Ed. (2020) 2–24, https://doi.org/10.1002/anie.202001876.
[2] F. Hollmann, I.W.C.E. Arends, D. Holtmann, Enzymatic reductions for the chemist, Green Chem. 13 (2011) 2285–2314, https://doi.org/10.1039/c1gc15424a.
[3] H.S. Toogood, N.S. Scrutton, Discovery, characterization, engineering, and applications of ene-reductases for industrial biocatalysis, ACS Catal. 8 (2018) 3532–3549, https://doi.org/10.1021/acscatal.8b00624.
[4] R.E. Williams, N.C. Bruce, 'New uses for an old enzyme'–the old yellow enzyme family of flavoenzymes, Microbiology 148 (2002) 1607–1614.
[5] R. Stuermer, B. Hauer, M. Hall, K. Faber, Asymmetric bioreduction of activated C═C bonds using enoate reductases from the old yellow enzyme family, Curr. Opin. Chem. Biol. 11 (2007) 203–213, https://doi.org/10.1016/j.cbpa.2007.02.025.
[6] C.K. Winkler, K. Faber, M. Hall, Biocatalytic reduction of activated C═C—bonds and beyond: emerging trends, Curr. Opin. Chem. Biol. 43 (2018) 97–105, https://doi.org/10.1016/j.cbpa.2017.12.003.
[7] N.B. Johnson, I.C. Lennon, P.H. Moran, J.A. Ramsden, Industrial-scale synthesis and applications of asymmetric hydrogenation catalysts, Acc. Chem. Res. 40 (2007) 1291–1299, https://doi.org/10.1021/ar700114k.
[8] T. Reß, W. Hummel, S.P. Hanlon, H. Iding, H. Gröger, The organic-synthetic potential of recombinant ene reductases: substrate-scope evaluation and process optimization, ChemCatChem. 7 (2015) 1302–1311, https://doi.org/10.1002/cctc.201402903.
[9] D. Mangan, I. Miskelly, T.S. Moody, A three-enzyme system involving an ene-reductase for generating valuable chiral building blocks, Adv. Synth. Catal. 354 (2012) 2185–2190, https://doi.org/10.1002/adsc.201101006.
[10] B. Dominguez, U. Schell, S. Bisagni, T. Kalthoff, Reduction of activated carbon-carbon double bonds using highly active and enantioselective double bond reductases ENEs from Johnson Matthey's enzyme collection provide a suitable alternative to metal-catalysed hydrogenation, Johnson Matthey Technol. Rev. 60 (2016) 243–249, https://doi.org/10.1595/205651316X692572.
[11] D.J. Bougioukou, A.Z. Walton, J.D. Stewart, Towards preparative-scale, biocatalytic alkene reductions, Chem. Commun. 46 (2010) 8558, https://doi.org/10.1039/c0cc03119d.
[12] C. Mähler, C. Burger, F. Kratzl, D. Weuster-Botz, K. Castiglione, Asymmetric whole-cell bio-reductions of (R)-carvone using optimized ene reductases, Molecules 24 (2019) 2550, https://doi.org/10.3390/molecules24142550.
[13] L. Zheng, J. Lin, B. Zhang, Y. Kuang, D. Wei, Identification of a yeast old yellow enzyme for highly enantioselective reduction of citral isomers to (R)-citronellal, Bioresour. Bioprocess. 5 (2018), https://doi.org/10.1186/s40643-018-0192-x.
[14] C. Stueckler, M. Hall, H. Ehammer, E. Pointner, W. Kroutil, P. Macheroux, K. Faber, Stereocomplementary bioreduction of alpha,beta-unsaturated dicarboxylic acids and dimethyl esters using enoate reductases: enzyme- and substrate-based stereocontrol, Org. Lett. 9 (2007) 5409–5411, https://doi.org/10.1021/ol7019185.
[15] M. Hall, C. Stueckler, H. Ehammer, E. Pointner, G. Oberdorfer, K. Gruber, B. Hauer, R. Stuermer, W. Kroutil, P. Macheroux, K. Faber, Asymmetric bioreduction of C═C bonds using enoate reductases OPR1, OPR3 and YqjM: enzyme-based stereocontrol, Adv. Synth. Catal. 350 (2008) 411–418, https://doi.org/10.1002/adsc.200700458.
[16] A. Scholtissek, D. Tischler, A. Westphal, W. van Berkel, C. Paul, Old yellow enzyme-catalysed asymmetric hydrogenation: linking family roots with improved catalysis, Catalysts 7 (2017) 130, https://doi.org/10.3390/catal7050130.
[17] G. Oberdorfer, K. Gruber, K. Faber, M. Hall, Stereocontrol strategies in the asymmetric bioreduction of alkenes, Synlett 23 (2012) 1857–1864, https://doi.org/10.1055/s-0032-1316591.
[18] D.J. Bougioukou, J.D. Stewart, Opposite stereochemical courses for enzyme-mediated alkene reductions of an enantiomeric substrate pair, J. Am. Chem. Soc. 130 (2008) 7655–7658, https://doi.org/10.1021/ja800200r.
[19] S.K. Padhi, D.J. Bougioukou, J.D. Stewart, Site-saturation mutagenesis of tryptophan 116 of Saccharomyces pastorianus old yellow enzyme uncovers stereocomplementary variants, J. Am. Chem. Soc. 131 (2009) 3271–3280, https://doi.org/10.1021/ja8081389.
[20] Q. Shi, H. Wang, J. Liu, S. Li, J. Guo, H. Li, X. Jia, H. Huo, Z. Zheng, S. You, B. Qin, Old yellow enzymes: structures and structure-guided engineering for stereocomplementary bioreduction, Appl. Microbiol. Biotechnol. 104 (2020) 8155–8170, https://doi.org/10.1007/s00253-020-10845-z.
[21] N. Kress, J. Rapp, B. Hauer, Enantioselective reduction of citral isomers in NCR ene reductase: analysis of an active-site mutant library, ChemBioChem. 18 (2017) 717–720, https://doi.org/10.1002/cbic.201700011.
[22] E.D. Amato, J.D. Stewart, Applications of protein engineering to members of the old yellow enzyme family, Biotechnol. Adv. 33 (2015) 624–631, https://doi.org/10.1016/j.biotechadv.2015.04.011.
[23] Y.A. Pompeu, B. Sullivan, J.D. Stewart, X-ray crystallography reveals how subtle changes control the orientation of substrate binding in an alkene reductase, ACS Catal. 3 (2013) 2376–2390, https://doi.org/10.1021/cs400622e.
[24] N. Nett, S. Duewel, A.A. Richter, S. Hoebenreich, Revealing additional stereocomplementary pairs of old yellow enzymes by rational transfer of engineered residues, ChemBioChem. 18 (2017) 685–691, https://doi.org/10.1002/cbic.201600688.
[25] T. Reignier, V. de Berardinis, J.-L. Petit, a Mariage, K. Hamzé, K. Duquesne, V. Alphand, Broadening the scope of Baeyer-Villiger monooxygenase activities toward α,β-unsaturated ketones: a promising route to chiral enol-lactones and ene-lactones, Chem. Commun. 21 (2014) 3–6, https://doi.org/10.1039/c4cc02541e.
[26] T.B. Fitzpatrick, N. Amrhein, P. Macheroux, Characterization of YqjM, an old yellow enzyme homolog from Bacillus subtilis involved in the oxidative stress response, J. Biol. Chem. 278 (2003) 19891–19897, https://doi.org/10.1074/jbc.M211778200.
[27] E. Vázquez-Figueroa, J. Chapparro-Riggers, A.S. Bommarius, Development of a thermostable glucose dehydrogenase by a structure-guided consensus concept, ChemBioChem 8 (2007) 2295–2301, https://doi.org/10.1002/cbic.200700500.
[28] A.G.W. Leslie, H.R. Powell, Processing Diffraction Data with MOSFLM, 2007, https://doi.org/10.1007/978-1-4020-6316-9_4.
[29] P. Evans, Scaling and assessment of data quality, Acta Crystallogr. Sect. D Biol. Crystallogr. 62 (2006) 72–82, https://doi.org/10.1107/S0907444905036693.
[30] A.J. McCoy, R.W. Grosse-Kunstleve, P.D. Adams, M.D. Winn, L.C. Storoni, R. J. Read, Phaser crystallographic software, J. Appl. Crystallogr. 40 (2007) 658–674, https://doi.org/10.1107/S0021889807021206.
[31] P. Emsley, B. Lohkamp, W.G. Scott, K. Cowtan, Features and development of coot, Acta Crystallogr. Sect. D Biol. Crystallogr. 66 (2010) 486–501, https://doi.org/10.1107/S0907444910007493.
[32] G.N. Murshudov, P. Skubák, A.A. Lebedev, N.S. Pannu, R.A. Steiner, R.A. Nicholls, M.D. Winn, F. Long, A.A. Vagin, REFMAC 5 for the refinement of macromolecular crystal structures, Acta Crystallogr. Sect. D Biol. Crystallogr. 67 (2011) 355–367, https://doi.org/10.1107/S0907444911001314.
[33] M.D. Winn, C.C. Ballard, K.D. Cowtan, E.J. Dodson, P. Emsley, P.R. Evans, R. M. Keegan, E.B. Krissinel, A.G.W. Leslie, A. McCoy, S.J. McNicholas, G. N. Murshudov, N.S. Pannu, E.A. Potterton, H.R. Powell, R.J. Read, A. Vagin, K. S. Wilson, Overview of the CCP 4 suite and current developments, Acta Crystallogr. Sect. D Biol. Crystallogr. 67 (2011) 235–242, https://doi.org/10.1107/S0907444910045749.
[34] D.J. Opperman, B.T. Sewell, D. Litthauer, M.N. Isupov, J.A. Littlechild, E. van Heerden, Crystal structure of a thermostable old yellow enzyme from Thermus scotoductus SA-01, Biochem. Biophys. Res. Commun. 393 (2010) 426–431, https://doi.org/10.1016/j.bbrc.2010.02.011.
[35] K. Shimoda, N. Kubota, H. Hamada, Asymmetric reduction of α,β-unsaturated carbonyl compounds with reductases from Nicotiana tabacum, Tetrahedron Asymmetry 15 (2004) 2443–2446, https://doi.org/10.1016/j.tetasy.2004.07.011.
[36] C.E. Paul, S. Gargiulo, D.J. Opperman, I. Lavandera, V. Gotor-Fernández, V. Gotor, A. Taglieber, I.W.C.E. Arends, F. Hollmann, Mimicking nature: synthetic nicotinamide cofactors for C═C bioreduction using enoate reductases, Org. Lett. 15 (2013) 180–183, https://doi.org/10.1021/ol303240a.

[37] S. Litthauer, S. Gargiulo, E. van Heerden, F. Hollmann, D.J. Opperman, Heterologous expression and characterization of the ene-reductases from Deinococcus radiodurans and Ralstonia metallidurans, J. Mol. Catal., B Enzym. 99 (2014) 89–95, https://doi.org/10.1016/j.molcatb.2013.10.020.
[38] D.J. Bougioukou, S. Kille, A. Taglieber, M.T. Reetz, Directed evolution of an enantioselective enoate-reductase: testing the utility of iterative saturation mutagenesis, Adv. Synth. Catal. 351 (2009) 3287–3305, https://doi.org/10.1002/adsc.200900644.
[39] M.W. Fraaije, A. Mattevi, Flavoenzymes: diverse catalysts with recurrent features, Trends Biochem. Sci. 25 (2000) 126–132, https://doi.org/10.1016/S0968-0004(99)01533-9.
[40] A.Z. Walton, W.C. Conerly, Y. Pompeu, B. Sullivan, J.D. Stewart, Biocatalytic reductions of Baylis–Hillman adducts, ACS Catal. 1 (2011) 989–993, https://doi.org/10.1021/cs200223f.
[41] R. Lonsdale, M.T. Reetz, Reduction of α,β-unsaturated ketones by old yellow enzymes: mechanistic insights from quantum mechanics/molecular mechanics calculations, J. Am. Chem. Soc. 137 (2015) 14733–14742, https://doi.org/10.1021/jacs.5b08687.
[42] J.T. Wu, L.H. Wu, J.A. Knight, Stability of NADPH: effect of various factors on the kinetics of degradation materials and methods, Clin. Chem. Clin. Chem. 32232 (1986) 314–319.
[43] V. Kaswurm, W. Van Hecke, K.D. Kulbe, R. Ludwig, Guidelines for the application of NAD(P)H regenerating glucose dehydrogenase in synthetic processes, Adv. Synth. Catal. 355 (2013) 1709–1714, https://doi.org/10.1002/adsc.201200959.
[44] E. Vazquez-Figueroa, V. Yeh, J.M. Broering, J.F. Chaparro-Riggers, A. S. Bommarius, Thermostable variants constructed via the structure-guided consensus method also show increased stability in salts solutions and homogeneous aqueous-organic media, Protein Eng. Des. Sel. 21 (2008) 673–680, https://doi.org/10.1093/protein/gzn048.
[45] J. Bernard, E. van Heerden, I.W.C.E. Arends, D.J. Opperman, F. Hollmann, Chemoenzymatic reduction of conjugated C=C double bonds, ChemCatChem. 4 (2012) 196–199, https://doi.org/10.1002/cctc.201100312.
[46] L. Kulishova, K. Dimoula, M. Jordan, A. Wirtz, D. Hofmann, B. Santiago-Schübel, J. Fitter, M. Pohl, A.C. Spiess, Factors influencing the operational stability of NADPH-dependent alcohol dehydrogenase and an NADH-dependent variant thereof in gas/solid reactors, J. Mol. Catal., B Enzym. 67 (2010) 271–283, https://doi.org/10.1016/j.molcatb.2010.09.005.
[47] A. Fryszkowska, H. Toogood, M. Sakuma, J. Gardiner, G. Stephens, N. Scrutton, Asymmetric reduction of activated alkenes by pentaerythritol tetranitrate reductase: specificity and control of stereochemical outcome by reaction optimisation, Adv. Synth. Catal. 351 (2009) 2976–2990, https://doi.org/10.1002/adsc.200900574.
[48] Y. Fu, K. Castiglione, D. Weuster-Botz, Comparative characterization of novel ene-reductases from cyanobacteria, Biotechnol. Bioeng. 110 (2013) 1293–1301, https://doi.org/10.1002/bit.24817.
[49] C. Stueckler, N.J. Mueller, C.K. Winkler, S.M. Glueck, K. Gruber, G. Steinkellner, K. Faber, Bioreduction of alpha-methylcinnamaldehyde derivatives: chemo-enzymatic asymmetric synthesis of Lilial and Helional, Dalton Trans. 39 (2010) 8472–8476, https://doi.org/10.1039/c002971h.
[50] Y. Yanto, C.K. Winkler, S. Lohr, M. Hall, K. Faber, A.S. Bommarius, Asymmetric bioreduction of alkenes using ene-reductases YersER and KYE1 and effects of organic solvents, Org. Lett. 13 (2011) 2540–2543, https://doi.org/10.1021/ol200394p.
[51] M. Bechtold, E. Brenna, C. Femmer, F.G. Gatti, S. Panke, F. Parmeggiani, A. Sacchetti, Biotechnological development of a practical synthesis of ethyl (S)-2-ethoxy-3-(p -methoxyphenyl)propanoate (EEHP): over 100-fold productivity increase from yeast whole cells to recombinant isolated enzymes, Org. Process Res. Dev. 16 (2012) 269–276, https://doi.org/10.1021/op200085k.
[52] B.V. Adalbjörnsson, H.S. Toogood, A. Fryszkowska, C.R. Pudney, T.A. Jowitt, D. Leys, N.S. Scrutton, Biocatalysis with thermostable enzymes: structure and properties of a thermophilic' ene'-reductase related to old yellow enzyme, ChemBioChem 11 (2010) 197–207, https://doi.org/10.1002/cbic.200900570.
[53] Y. Wang, M.J. Bartlett, C.A. Denard, J.F. Hartwig, H. Zhao, Combining Rh-Catalyzed diazocoupling and enzymatic reduction to efficiently synthesize enantioenriched 2-Substituted succinate derivatives, ACS Catal. 7 (2017) 2548–2552, https://doi.org/10.1021/acscatal.7b00254.
[54] H. Gröger, W. Hummel, Combining the "two worlds" of chemocatalysis and biocatalysis towards multi-step one-pot processes in aqueous media, Curr. Opin. Chem. Biol. 19 (2014) 171–179, https://doi.org/10.1016/j.cbpa.2014.03.002.
[55] J.H. Schrittwieser, S. Velikogne, M. Hall, W. Kroutil, Artificial biocatalytic linear cascades for preparation of organic molecules, Chem. Rev. 118 (2018) 270–348, https://doi.org/10.1021/acs.chemrev.7b00033.